Optimized PARACEST Signal Detection by Echo-Planar Imaging

A. E. Campbell[1,2], A. Li[1], C. Jones[1,3], and R. Bartha[1]

[1]Centre for Functional and Metabolic Mapping, Robarts Research Institute, University of Western Ontario, London, Ontario, Canada, [2]Centre for Advanced Biomedical Imaging, University College London, London, Greater London, United Kingdom, [3]F.M. Kirby Research Center for Functional Brain Imaging, Kennedy Krieger Institute, John Hopkins University, Baltimore, Maryland, United States

Introduction: Paramagnetic chemical exchange saturation transfer (PARACEST) agents are being developed for in-vivo magnetic resonance imaging (MRI) [1,2]. These agents are sensitive to physiological parameters such as pH and temperature. PARACEST agents produce contrast by the selective saturation and exchange of agent-bound protons with bulk water protons. However, in-vivo, the magnetization transfer from endogenous macromolecules can interfere with the performance of the PARACEST agent unless the exchangeable agent bound protons have very large chemical shift (>150ppm from the bound water pool) [3]. The agents may also modify the relaxation rates of bulk water, decreasing the isolated PARACEST contrast obtained in-vivo [4]. The purpose of this study was to develop an MRI simulator to explore and optimize Echo-Planar Imaging (EPI) sequences for in-vivo PARACEST detection. The MRI simulation techniques were required to accurately replicate in-vivo imaging conditions. An optimal dynamic EPI scheme was developed to isolate PARACEST detection with feasible signal-to-noise ratio (SNR) for detection of the agent Dy^{3+}-DOTAM-GlyLys.

Methods: The MR image simulator was developed by numerically solving a four-pool Bloch equation model incorporating chemical exchange [3] step-wise through the pulse sequence for each pixel in the image. Two-dimensional Gaussian noise was added to k-space to produce a pre-determined SNR in image-space. The accuracy of the simulation software was verified by comparison to experimental data for a FLASH sequence (results not shown). The multi-shot EPI sequence (FOV=30 mm x 30 mm, α=25°, TR=8.55ms, B_1=30 µT) designed for PARACEST detection incorporated an off-resonance saturation pulse prior to each alpha pulse. EPI sequences were optimized by modeling the detection of water bound to Dy^{3+}-DOTAM-GlyLys (bound water shift = -720ppm, bound water lifetime = 17 µs). Two conditions were simulated: 1) PARACEST agent in a 10% cross-linked bovine serum albumin (BSA) solution and 2) 10% cross-linked BSA solution, to represent tissue with and without PARACEST agent present. To reduce computation time, experiments were performed using a 32x32 resolution (Figure 1). The homogeneous center region within each vial was chosen for region-of-interest (ROI) calculations of *%CEST* = (1-SI_{bound_water}/SI_{-bound_water})x100, where *SI* is the mean signal intensity, the subscript represents saturation frequency. The saturation times and number of shots used to form an image were optimized. An alternating ("on"/"off") acquisition scheme was tested by simulating the acquisition of multiple images acquired in series with 3s delay between acquisitions. The "on" case represents images in which the bound water pool was saturated, while the "off" condition represents a control image where the negative of the bound water pool was saturated. A left-tailed student's paired t-test ($p<0.05$) was used to compare the "on" state to the "off" state for each pixel, to identify pixels with significant change in signal intensity. PARACEST detection was defined as present if >50% of the pixels in the agent-containing region showed a statistically significant signal change. The number of "on" and "off" images in series and the number of repetitions of the "on" / "off" pattern were varied to find the minimum SNR required to achieve detection for Dy^{3+}-DOTAM-GlyLys at concentrations of 1 mM and 100 µM.

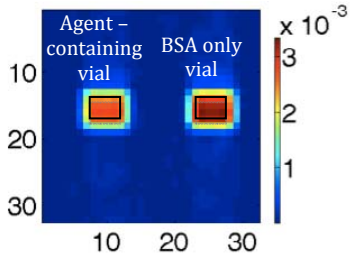

Figure 1: Experimental setup for simulations. The black outlines represent the ROIs for analysis

Results and Discussion:

The CEST effect was independent of the number of shots (Figure 2 for 1mM). Therefore, an 8-shot EPI sequence was chosen for further testing. Increasing the pre-saturation pulse length increased *%CEST* effect (Figure 3 for 1mM) as expected, so 10s was chosen for the simulation of time-course acquisitions. The minimum SNR required to achieve detection for a number of different time-course configurations is shown in Figure 4. The required SNR for detection was much lower for the 1 mM case compared to the 100 µM case as expected. The optimal alternating acquisition scheme contained 2-4 images in series (Figure 4a) when using 4 repetitions. Increasing the number of repetitions of the "on" / "off" pattern also decreased the minimum SNR for detection (Figure 4b) when using 2 and 4 images in series (for 100µM and 1mM, respectively). The SNR required for detection, even for 100 µM concentration is experimentally achievable (<200) using the highly efficient EPI acquisition scheme. Based on the simulation results, the isolated *%CEST* for the 100 µM and 1mM concentrations were calculated to be: 0.81% and 3.52% (respectively) for the EPI sequence.

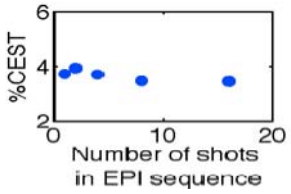

Figure 2: Effect of the number of shots in the EPI sequence

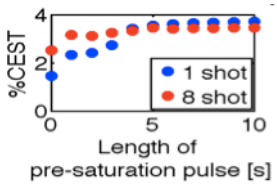

Figure 3: Pre-saturation pulse length

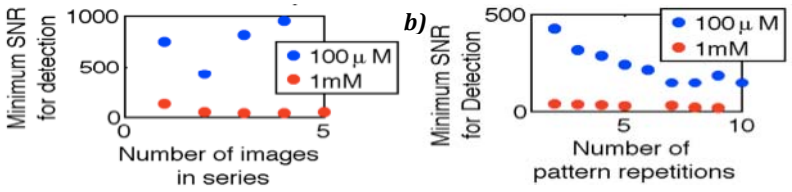

Figure 4: Detection SNR required varying the number of "on"/ "off" images in a row (a) and repetitions of the "on"/"off" pattern (b)

Conclusion: The MRI EPI simulator developed in this study was used to optimize the detection scheme for PARACEST contrast agents in-vivo. Image simulation is a useful investigation tool, which minimizes time required on the MRI scanner. The results indicate that the highly efficient EPI sequence may have considerable advantages for the in-vivo detection of PARACEST contrast due to the very rapid imaging time. The "on" / "off" acquisition scheme improved detection sensitivity in the presence of noise. Detection of 100 µM Dy^{3+}-DOTAM-GlyLys will require SNR ~200.

References: [1] Zhang et al, *Journal of the American Chemical Society* **123** (7): 1517-18 (2001). [2] Aime et al, *Magnetic Resonance in Medicine* **47**(4): 639-648 (2002). [3] Li et al, *Magnetic Resonance in Medicine* **60** (5):1197–1206 (2008). [4] Ward et al, *Journal of Magnetic Resonance* **143** (1):79-87 (2000).